Mode-locked biphoton generation by concurrent quasi-phase-matching

Y. F. Bai,[1] P. Xu,[1,*] Z. D. Xie,[1] Y. X. Gong,[2] and S. N. Zhu[1]

[1]*National Laboratory of Solid State Microstructures and School of Physics, Nanjing University, Nanjing, 210093, China*

[2]*Physics Department, Southeast University, Nanjing, 211189, China*

(Received 16 October 2011; published 7 May 2012)

We report a scheme for mode-locked biphoton generation by engineering quasi-phase-matching materials. An aperiodically poled lithium tantalate is designed to supply multiple reciprocal vectors for two-photon frequency comb generation. Temporally, such two-photon state exhibits mode-locked pulse train. The two-photon pulse duration reaches 4.2 fs when the frequency comb is centered at 800 nm and covers 442 nm. The HOM interference of the mode-locked biphoton approaches a 1.26-μm dip and exhibits a reappearance of dip and peak, which can be taken as a new scheme for engineering quantum light source. Furthermore, we also design another aperiodically poled crystal to generate two sets of frequency combs. The HOM interference will appear as a revival of spatial beatings. The mode-locked biphotons suggest applications in precise time synchronization, quantum metrology, quantum optical coherence tomography, and quantum computing.

DOI: 10.1103/PhysRevA.85.053807 PACS number(s): 42.65.Lm, 42.50.Dv, 03.65.Ud, 42.50.Ar

Entangled photons lie at the heart of quantum information science and technology. A widely used method to generate entangled photons is spontaneous parametric down-conversion (SPDC) [1,2] in nonlinear optical crystals. Among them quasi-phase-matching (QPM) crystals play important roles in efficient generation of entangled photons as well as the manipulation of spatial [3–5] and frequency entanglement [6–9]. By designing chirped quasi-phase-matching nonlinear crystals [6–8], several groups focus on broadband two-photon generation and have achieved an ultrashort temporal correlation toward single-cycle limit, which is extraordinarily useful in clock synchronization [10], quantum metrology [11], and quantum optical coherence tomography [12].

An alternative way to achieve the broadband spectrum is engineering the frequency comb, which is the working principle of classical mode-locked laser. The two-photon frequency comb should have equivalent applications in quantum optics, like a continuous broadband spectrum, but the brightness of each mode will be much higher. Ou [13] first reported a two-photon frequency comb by using Fabry-Perot cavity after the entangled photons were generated. In that work, the frequency spacing is concerned with the cavity round trip and the total bandwidth of frequency comb is determined by the spectrum of SPDC process. In this work we aim to engineer the broadband optical frequency comb at the source. The mode-locked two-photon state is directly generated from an aperiodically poled nonlinear crystal (APNC). The mode spacing can be any value as we designed and the time correlation of such mode-locked biphoton exhibits as a pulse train. Each correlation peak reaches single cycle when the bandwidth of frequency comb is close to the central frequency. By designing another different set of reciprocal vectors of APNC, we can obtain two sets of frequency combs and achieve a new type of mode-locked two-photon state. We design the HOM interferometer to investigate the mode-locked biphotons. Serving as a new scheme for single-cycle biphoton preparation, the optical material engineering can be applied for exploiting new types of quantum light source, studying nonlinear optical process at single photon level and playing an important role in quantum computing [14–16].

For a periodically poled nonlinear crystal, usually only a single reciprocal vector is used to support a degenerate or nondegenerate photon pair generation by satisfying the phase matching condition $\Delta k = k_p - k_s - k_i - g = 0$. For frequency comb biphoton generation, we use an aperiodically poled nonlinear crystal, which can supply multiple reciprocal vectors to satisfy multiple spontaneous down-conversions concurrently. The poling function [17] can be written as

$$\chi^{(2)}(z) = \chi^{(2)}\mathrm{sgn}\left[\sum_n a_n \cos(g_n z + \phi_n)\right], \tag{1}$$

where g_n is the nth reciprocal vector, a_n and ϕ_n are adjustable parameters representing amplitude and phase for each g_n, respectively. $\chi^{(2)}$ is the second-order nonlinearity of the material. By our design, all amplitudes a_n are equal and all reciprocal vectors are in phase with $\phi_n = 0$. Theoretically, the cosine poling function can provide the maximum Fourier coefficient for each g_n to ensure a most efficient quasi-phase-matching process. However, from the viewpoint of practical engineering, the crystals such as lithium tantalate and lithium niobate can only be poled via periodic reversion of domains, which will reduce the effective nonlinearity. For a periodically poled nonlinear crystal, the maximum achievable Fourier coefficient for the designed reciprocal vector is $2/\pi$. Figure 1 shows how to design the domain structure where three SPDC processes are mixed.

Here we design N reciprocal vectors for N concurrent SPDC processes. Each generated frequency pair is taken as a mode and all modes are equally spaced. If all the modes are in coherent superposition, mode-locked two-photon will be generated. The interaction Hamilton inside the APNC can be written as

$$\hat{H} = \epsilon_0 \sum_n \int d\vec{r}\, \chi_n^{(2)} e^{-i g_n z} \hat{E}_p^{(+)} \hat{E}_s^{(-)} \hat{E}_i^{(-)} + \mathrm{H.c.} \tag{2}$$

*pingxu520@nju.edu.cn

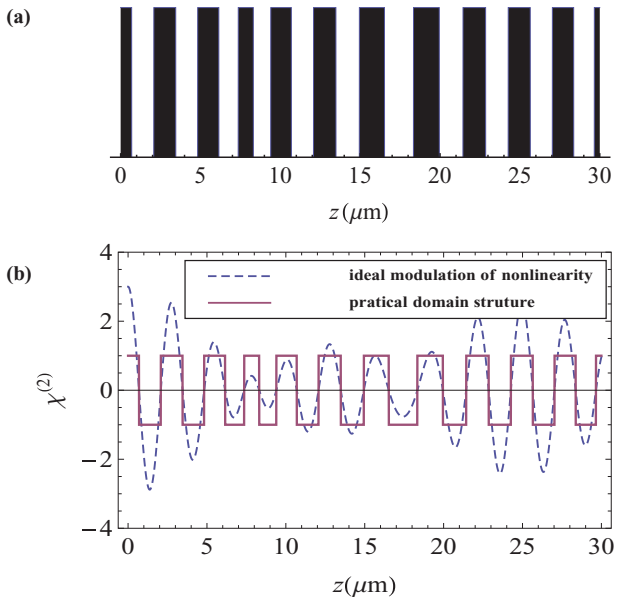

FIG. 1. (Color online) Design of the APNC structure. (a) The domain structure of APNC. (b) Comparison between ideal modulation of nonlinearity and practical domain structure.

Considering the first-order perturbation approximation, we can derive the wave function

$$|\psi\rangle_{ML} = \psi_0 \sum_{n=1}^{N} \int d\nu \mathrm{sinc}\left(\frac{1}{2}\nu D_n L\right) \hat{a}_{s_n}^{\dagger} \hat{a}_{i_n}^{\dagger} |0\rangle. \quad (3)$$

Since we design a constant amplitude for each g_n, then $\chi_n^{(2)}$ can be considered as a constant $\chi_{\mathrm{eff}}^{(2)}$. In the above equation, $\psi_0 = \frac{\chi_{\mathrm{eff}}^{(2)} E_p L}{2V_Q n_s n_i} \sqrt{\omega_s \omega_i}$, which includes all the constants and slowly varying terms. N is the total number of frequency pairs. ν is the the detuning frequency around the center frequency. $D_n = \frac{1}{u_{s_n}} - \frac{1}{u_{i_n}}$ is the group velocity dispersion of the nth frequency pair and L is the crystal length. For each frequency pair of the two-photon state, we have $\omega_p = \omega_{s_n} + \omega_{i_n}$. Suppose $\Omega_{s_n}, \Omega_{i_n}$ are the central frequency of each frequency pair, then we have $\omega_{s_n} = \Omega_{s_n} + \nu$, $\omega_{i_n} = \Omega_{i_n} - \nu$. Suppose $\Delta\omega$ is the mode spacing, then $\Omega_{s_n} = \Omega_s + n\Delta\omega$, $\Omega_{i_n} = \Omega_i - n\Delta\omega$, in which Ω_s and Ω_i indicate the central frequency of the frequency pair most close to the degenerate frequency. As we only consider the temporal correlation, we neglect the spatial part of the wave function. Thus, the second-order time correlation function is calculated to be

$$G^{(2)}(\tau_1, \tau_2) \propto \left| \sum_{n=1}^{N} e^{-i\omega_p \frac{\tau_1+\tau_2}{2}} e^{-i\frac{\Omega_{d_n}}{2}\tau} \mathrm{rect}\left(\frac{2\tau}{D_n L}\right) \right|^2, \quad (4)$$

where $\Omega_{d_n} = \Omega_{s_n} - \Omega_{i_n}$, $\tau = \tau_1 - \tau_2$. In the ideal case, we take all D_n as the same value D to simplify the two-photon time correlation function,

$$G^{(2)}(\tau) \propto \mathrm{rect}\left(\frac{2\tau}{DL}\right) \left[\frac{\sin\left(\frac{N\Delta\omega}{2}\tau\right)}{\sin\left(\frac{\Delta\omega}{2}\tau\right)}\right]^2. \quad (5)$$

For the photon pair with a single frequency pair, the time correlation function is a rectangle function in the form of $\mathrm{rect}(\frac{2\tau}{DL})$, whose width is determined by the group velocity dispersion and the crystal length. Usually the photon pairs generated from lithium tantalate are well synchronized by picosecond precision. However, in this work, different frequency modes are equally spaced which contributes an equidifferent phase to the time correlation function. Superposition and interference result in a temporally ultrashort pulse train in the form of $[\sin(\frac{N\Delta\omega}{2}\tau)/\sin(\frac{\Delta\omega}{2}\tau)]^2$. This is the physics behind the two-photon mode-locking. The width of two-photon correlation peaks is determined by the mode spacing and the number of frequency pairs. If the frequency comb covers as broadly as the central frequency, it will approach the level of femtosecond, i.e., a single-cycle. However, when discussing this we make an assumption that the group velocity dispersion for each frequency pair is taken to be constant, which is valid for some small dispersion materials, or the frequency comb covering not too broadly. We will give a specific discussion about it later.

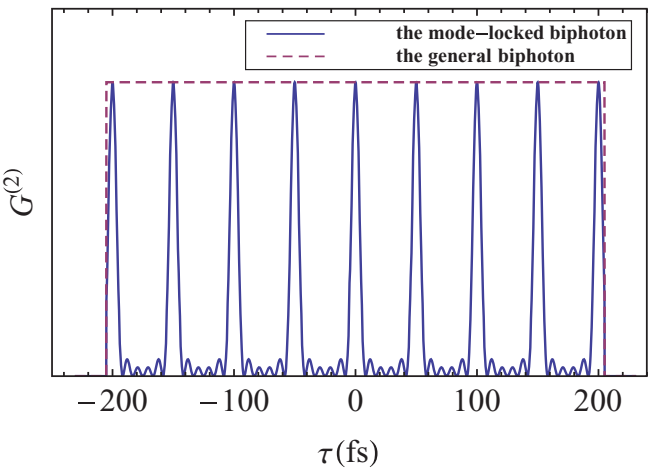

FIG. 2. (Color online) Comparison between time correlation of mode-locked biphotons from the APNC and that of the general biphotons from a single plain crystal.

In analogy with the mode-locked laser, the physics of mode-locked two-photon lies in that all the frequency pairs are in phase since they come from the same original pump photon and inherit the phase information. Besides, all reciprocal vectors are designed to be in phase. We have to emphasize that although the spectrum of signal or idler photon takes the form of frequency comb, neither the signal nor the idler photon is mode-locked due to the fact that the phase of single photon is random.

In our numerical calculation, we take $\lambda_p = 400$ nm, $\Delta\omega = 1.26 \times 10^{14}$ Hz, $L = 10$ mm, $N = 6$. The overall frequency comb covers 442 nm. The APNC is fabricated from a congruent lithium niobate (CLT) crystal. By using the Sellmeier equation of CLT, we can derive the magnitude of each reciprocal vector at 180° C: 2.1372 $\mu\mathrm{m}^{-1}$, 2.1269 $\mu\mathrm{m}^{-1}$, 2.1062 $\mu\mathrm{m}^{-1}$, 2.0752 $\mu\mathrm{m}^{-1}$, 2.0337 $\mu\mathrm{m}^{-1}$, 1.9816 $\mu\mathrm{m}^{-1}$. The two-photon then will be mode-locked to 4.2 fs as shown in Fig. 2. The rectangle time correlation function in Fig. 2 corresponds to the situation of 400 nm → 779 nm + 822 nm in a 10-mm-long crystal. We have to emphasize that in practical engineering we may choose the third-order reciprocal vectors working for the quasi-phase-matching conditions so as to ensure the homogeneity of the sample. Up to now, no single-photon

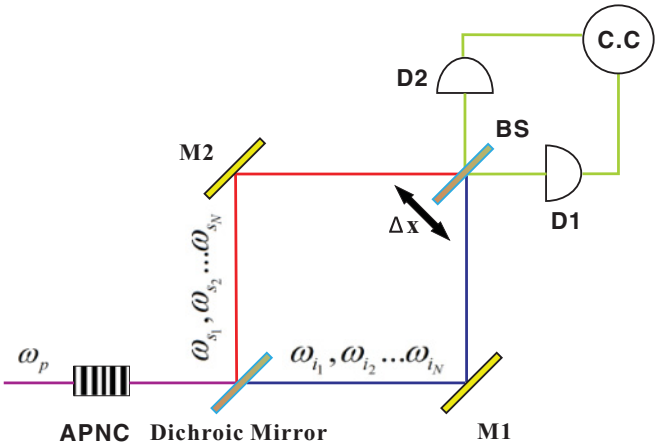

FIG. 3. (Color online) Schematic diagram of the HOM interferometer. A dichroic mirror is used to split the photon pair into two paths. The reflected signal photon and transmitted idler photon will be recombined together after passing through the beam splitter. Here we suppose the two single-photon detectors can respond to all the frequencies.

detectors can resolve the picosecond time duration. Instead of measuring the time correlation of such two-photon state directly, we can set up a HOM interferometer to reveal the mode-locked character. In Fig. 3, for a collinear type-I SPDC, mode-locked biphotons are separated by a dichroic mirror. Signal photons propagate along the reflected path while the idler photons propagate along the transmitted path. The beam splitter (BS) recombines the photon pair and two-photon interference will take place. The beam splitter is displaced from its symmetry position by changing small distances Δx. Both of the single-photon detectors can detect all the wavelengths of frequency comb. To be mentioned that, the optical path before the BS has to be accurately chosen to ensure that all the modes are in phase when they arrive at the BS.

The electromagnetic field operators at D_1 and D_2 are expressed by

$$\begin{aligned}\hat{E}_1^{(+)}(t_1,x_1) &= \sqrt{T}\hat{E}_{20}^{(+)} + i\sqrt{R}\hat{E}_{10}^{(+)}e^{i\omega_1\frac{\Delta x}{c}} \\ \hat{E}_2^{(+)}(t_2,x_2) &= \sqrt{T}\hat{E}_{10}^{(+)} + i\sqrt{R}\hat{E}_{20}^{(+)}e^{-i\omega_2\frac{\Delta x}{c}}.\end{aligned} \tag{6}$$

Then we can calculate the two-photon amplitude,

$$\begin{aligned}A(\tau_1,\tau_2) \propto e^{-i\omega_p\frac{\tau_1+\tau_2}{2}}e^{-i\Omega_d\frac{\Delta x}{c}}\Bigg[Tg(\tau) \\ -Re^{i\Omega_d\frac{\Delta x}{c}}g\left(\tau-2\frac{\Delta x}{c}\right)\Bigg],\end{aligned} \tag{7}$$

where $g(\tau) = \int d\nu\phi(\nu)e^{-i\nu\tau}$, $\phi(\nu)$ is the spectrum function of each mode, and $\Omega_d = \Omega_s - \Omega_i$. In our calculation, we take $T = R = \frac{1}{2}$ and suppose each mode has equal spectrum width $\sigma = 6.3 \times 10^{12}$ Hz.

There are N pairs of frequency modes. Each pair provides its two-photon amplitude $A_n(\tau)$. By summing all of them, we get the total two-photon amplitude $A(\tau)$. Then we can work out the coincidence counting rate by integrating $|A(\tau)|^2$ from $-\infty$ to $+\infty$,

$$R_{cc} = 1 - \frac{\sum_n \int d\tau g_n(\tau)g_n\left(\tau - 2\frac{\Delta x}{c}\right)cos\left(\Omega_{d_n}\frac{\Delta x}{c}\right)}{\sum_n \int d\tau g_n(\tau)^2}, \tag{8}$$

where we neglect the small contributions from terms $A_n(\tau)A_m^*(\tau)(m \neq n)$.

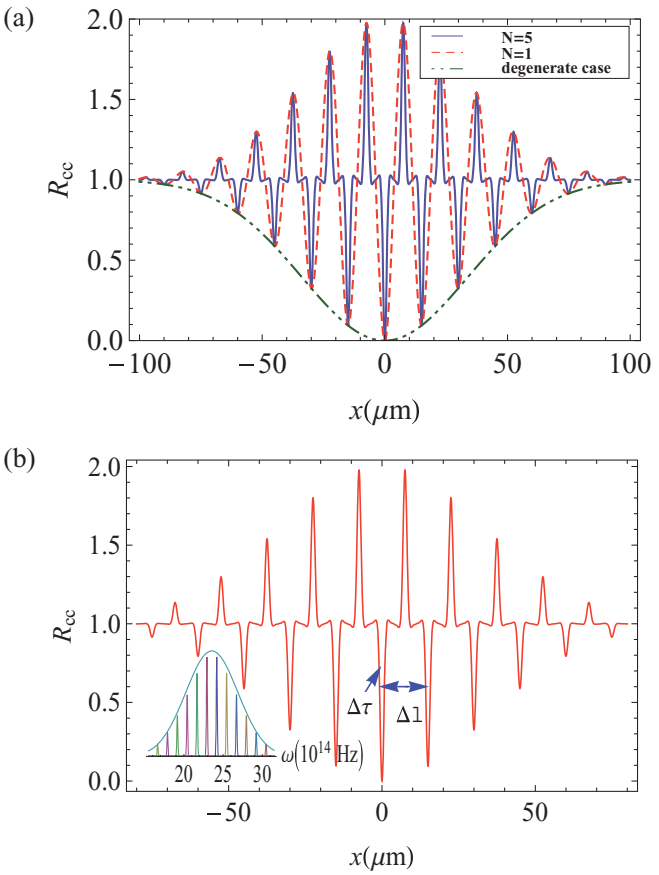

FIG. 4. (Color online) HOM interference pattern of mode-locked biphoton. (a) HOM interference pattern of mode-locked two-photon state for different number of frequency pairs. (b) HOM interference pattern of mode-locked two-photon state when the number of frequency pairs is 6. The inset is the corresponding frequency spectrum of optical frequency comb with Gaussian envelope.

By designing the APNC structure, we can get any desired spectrum envelope of frequency comb. In the following calculation, we consider all the frequency combs have a Gaussian envelope. By changing the number of frequency pairs, we obtain different results after the HOM interferometer. As shown in Fig. 4(a), the width of HOM dip is 48 μm when only one reciprocal vector takes the role for 800-nm degenerate photon pair generation. When another reciprocal vector contributes to the nondegenerate photon pair at 779 and 822 nm, we will see the beating inside the HOM dip as first reported in Ref. [18]. The beating frequency is 1.26×10^{14} Hz. Furthermore, when five pairs of nondegenerate frequency are taken into account, the HOM interference pattern turns out to be a series of narrow dips and peaks. When the FWHM of the frequency comb envelope is 242 nm ($N = 6$), each dip or peak covers 1.26 μm. This indicates that temporally

the two-photon is 4.2-fs mode-locked pulse. Narrower dip or narrower mode-locked two-photon pulse can be achieved when more frequency pairs are involved.

The width (FWHM) of each dip in Fig. 4(b) is determined by the bandwidth of frequency envelope. The dip width is written as

$$\Delta\tau \sim \frac{\pi}{N\Delta\omega}. \tag{9}$$

It is the equal mode spacing that causes the reappearance of the dip. Here the period for dip reappearance is 15 μm, which is associated with the mode spacing,

$$\Delta l \sim \frac{2c\pi}{\Delta\omega}. \tag{10}$$

For a traditional HOM interference, the dip or minimum coincidence rate can be understood as the results of two-photon interference. Photon pairs are bunched and captured two by two by either single-photon detector. A reversed HOM interferometer [19] will present correlation peak when two paths before the beam splitter have equal optical path. This means photon pair are more likely to be captured separately by two detectors and $|1,1\rangle$ state is dominant. Then what does the reappearance of peak and dip mean? We now analyze the two-photon state after the beam splitter,

$$|\psi\rangle = \sum_n \{(|2_a,0_b\rangle_n + e^{i\theta_n}|0_a,2_b\rangle_n) + i(|1_a,1_b\rangle_n - e^{i\theta_n}|1_b,1_a\rangle_n)\}, \tag{11}$$

where a, b indicate different optical paths. For each frequency pair, when $\theta_n = 0$, the correlation dip appears, while when $\theta_n = \pi$, the correlation peak emerges. In our case, θ_n can be written as

$$\theta_n = \frac{2n\Delta\omega\Delta x}{c}. \tag{12}$$

The superposition of different frequency pairs will lead to reappearance of the dip and peak when the BS is displaced at definite positions. Since θ changes with the optical path difference of HOM interferometer, dip and peak reappear periodically. By changing the optical path difference of the interferometer, we can engineer different quantum light source. It is worth mentioning that in addition to the HOM interferometer we can also use broadband sum-frequency-generation as an ultrafast correlator [8] to explore the temporal character of mode-locked biphotons.

A more general mode-locked biphoton state is that the photon pair covers two sets of frequency combs. The signal comb and idler comb both carrying Gaussian envelopes are separated away from the degenerate wavelength. We find a new character when observing the HOM interference as shown in Fig. 5. The coincidence counting rate between two detectors exhibits periodic revival, which is not the neat dip or peak but the spatial beating. The beating cycle is concerned with the difference of center mode of two frequency combs. This mode-locked two-photon with two separate frequency combs is first calculated here. In classical laser, no similar concepts can be referred to. Here we take $\lambda_p = 532$ nm,

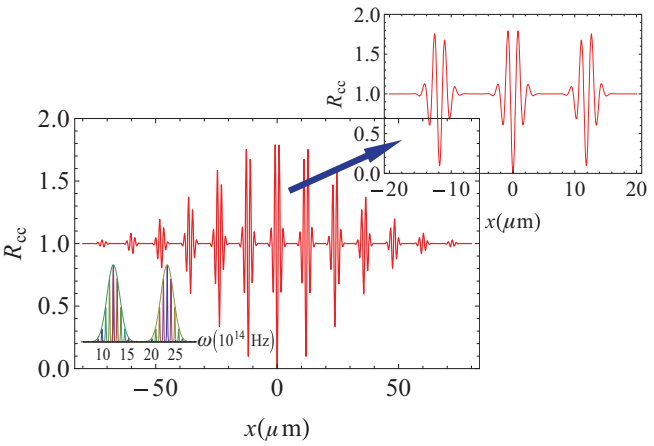

FIG. 5. (Color online) HOM interference pattern of mode-locked two-photon state, which covers two sets of frequency combs. The inset is the corresponding frequency spectrum when the signal comb and idler comb both carry Gaussian envelopes.

$\lambda_{s_0} = 810$ nm, $\lambda_{i_0} = 1550$ nm, $N = 9$, $\Delta\omega = 7.85 \times 10^{13}$ Hz and $\sigma = 7.85 \times 10^{12}$ Hz.

In the above discussions, we take the group velocity dispersion between signal and idler photons almost the same for each frequency pair. It comes to be true when we consider some materials with small group velocity dispersion and also for the case that the frequency comb is not too broad. Experimentally we can use a medium with the negative dispersion to compensate the dispersion. When taking the group velocity dispersion of CLT into the calculation of time correlation, we find the width of peak around $\tau = 0$ does not change and peaks elsewhere are broadened. The middle correlation peak corresponds to the situation when the optical path before BS is equal. The broadening effect cannot be eliminated because it is caused by the nonlinear crystal's intrinsic property. However, experimentally we are only concerned about central correlation peak, which is still well mode-locked. Another problem one may encounter in practical engineering is the poling of tiny domains when several different reciprocal vectors coexist. For a 0.5-mm-thick sample, the domains smaller than 2 μm can hardly be poled. To solve this problem, one may practically neglect the tiny domain and incorporate it with its adjacent domain. It will make the poling function deviate a little from the desired one, which can be considered as a fabrication error. It will broaden each frequency mode but affect little on the shape of the frequency comb. The narrow dip and peak of HOM interference will not change except the envelope of interference pattern will be varied. But such effects are not dominant since the possibility of finding tiny domains is not high.

A well-designed cascaded or multistripe periodically poled nonlinear crystal may be used to generate a two-photon frequency comb. However, extra efforts are required to make all the frequency modes in phase. For the cascaded periodically poled crystal, different frequency pairs are generated at different locations. Different modes propagate and would be out of phase, which will not result in a mode-locked biphoton from such crystals. For the multistripe

crystal, we have to make the photon pair from different stripes indistinguishable, such as using single-mode fiber to collect the photon pairs. So the scheme by use of APNC for mode-locked biphoton generation is compact and feasible.

In summary, we have proposed a scheme to generate mode-locked biphoton by designing the aperiodically poled nonlinear crystal with concurrent quasi-phase-matchings. We analyze the temporal correlation of two types of such states in virtue of the HOM interferometer. When the frequency comb is broadband, the ultrashort time correlation can reach single-cycle length, which is quite useful in a wide range of areas. Furthermore, when the signal and idler comb is nondegenerate, we find a reappearance of two-photon optical beating after HOM interferometer. The physics behind the results is the superposition of different frequency modes when they are in phase. The multiple frequency modes may carry diverse information, which would be of great use in quantum wavelength-division multiplexing. Besides, due to the high-dimensionality of frequency degree, shaping the spectrum of biphoton will benefit a wealth of physical phenomena and supply a new scheme for quantum-state engineering. Since optical frequency comb can be engineered as a large cluster state, which is the core of the one-way quantum computation scheme [14–16], the aperiodically poled nonlinear crystal may supply as a crucial component in this field.

ACKNOWLEDGMENTS

The authors thank Y. H. Shih and L. Yan for helpful discussions. This work was supported by the State Key Program for Basic Research of China (Grant Nos. 2012CB921802 and 2011CBA00205), the National Natural Science Foundations of China (Grant Nos. 10409066, 91121001, and 11021403), and the Project Funded by the Priority Academic Program Development of Jiangsu Higher Education Institutions (PAPD).

[1] Y. H. Shih and C. O. Alley, Phys. Rev. Lett. **61**, 2921 (1988).
[2] C. K. Hong, Z. Y. Ou, and L. Mandel, Phys. Rev. Lett. **59**, 2044 (1987).
[3] J. P. Torres, A. Alexandrescu, S. Carrasco, and L. Torner, Opt. Lett. **29**, 376 (2004).
[4] X. Q. Yu, P. Xu, Z. D. Xie, J. F. Wang, H. Y. Leng, J. S. Zhao, S. N. Zhu, and N. B. Ming, Phys. Rev. Lett. **101**, 233601 (2008).
[5] H. Y. Leng, X. Q. Yu, Y. X. Gong, P. Xu, Z. D. Xie, H. Jin, C. Zhang, and S. N. Zhu, Nature Commun. **2**, 429 (2011).
[6] S. E. Harris, Phys. Rev. Lett. **98**, 063602 (2007).
[7] M. B. Nasr, S. Carrasco, B. E. A. Saleh, A. V. Sergienko, M. C. Teich, J. P. Torres, L. Torner, D. S. Hum, and M. M. Fejer, Phys. Rev. Lett. **100**, 183601 (2008).
[8] S. Sensarn, G. Y. Yin, and S. E. Harris, Phys. Rev. Lett. **104**, 253602 (2010).
[9] A. M. Braänczyk, A. Fedrizzi, T. M. Stace, T. C. Ralph, and A. G. White, Opt. Express **19**, 55 (2011)
[10] A. Valencia, G. Scarcelli, and Y. Shih, Appl. Phys. Lett. **85**, 2655 (2004).
[11] V. Giovannetti, S. Lloyd, and L. Maccone, Science **306**, 1330 (2004).
[12] M. B. Nasr, B. E. A. Saleh, A. V. Sergienko, and M. C. Teich, Phys. Rev. Lett. **91**, 083601 (2003).
[13] Y. J. Lu, R. L. Campbell, and Z. Y. Ou, Phys. Rev. Lett. **91**, 163602 (2003).
[14] N. C. Menicucci, S. T. Flammia, and O. Pfister, Phys. Rev. Lett. **101**, 130501 (2008).
[15] M. Pysher, Y. Miwa, R. Shahrokhshahi, R. Bloomer, and O. Pfister, Phys. Rev. Lett. **107**, 030505 (2011).
[16] M. Pysher, A. Bahabad, P. Peng, A. Arie, and O. Pfister, Opt. Lett. **35**, 565 (2010).
[17] A. Norton and C. de Sterke, Opt. Express **12**, 841 (2004).
[18] Z. Y. Ou and L. Mandel, Phys. Rev. Lett. **61**, 54 (1988).
[19] J. Chen, K. F. Lee, and P. Kumar, Phys. Rev. A **76**, 031804 (2007).